Feasibility studies of the $\bar{p}p \rightarrow \pi^0 e^+ e^-$ electromagnetic channel at $\bar{\text{P}}$ANDA

Jérôme Boucher

January, 12th 2012

Outline

I. Physics motivations: the proton electromagnetic form factors
II. Model for $\bar{p}p \rightarrow \pi^0 e^+ e^-$
III. Hadronic tensor extraction
IV. Proton electromagnetic form factor extraction
V. Conclusion and outlook

Accessing the proton electromagnetic FFs

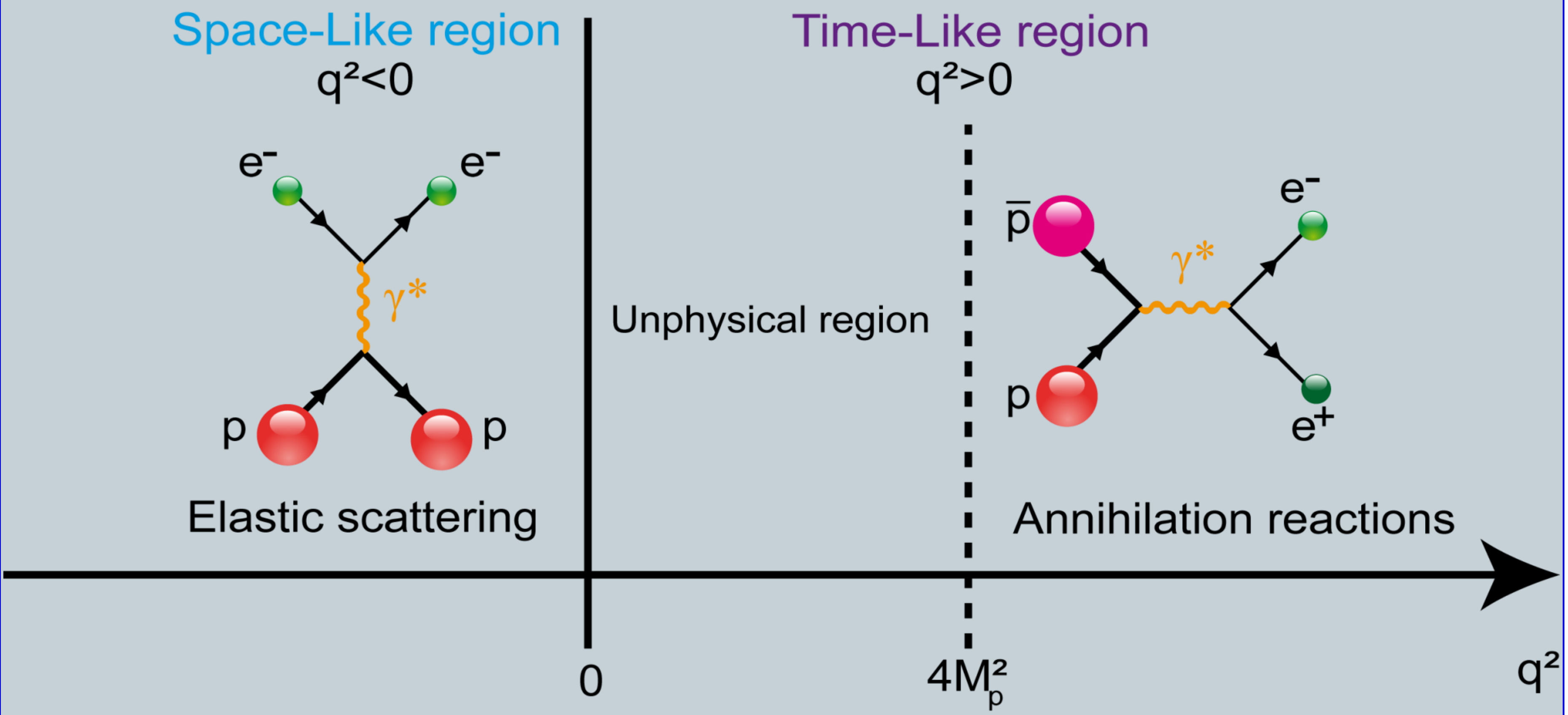

Proton electromagnetic FFs world data

Phragmén-Lindelhöf theorem:

$$\lim_{q^2\to-\infty} G_{E,M}(q^2) = \lim_{q^2\to+\infty} G_{E,M}(q^2)$$

Asymptotics:

$$\lim_{q^2\to\pm\infty}\left|G_{E,M}^{SL,TL}\left(q^2\right)\right| = \left(q^2\right)^{-2}$$

$G_E(4M_p^2)=G_M(4M_p^2)$

$G_E(0)=1$

$G_M(0)=\mu^p/\mu^N$

Sudoł et al., EPJA 44, 473-384 (2010)

Expected precision on G_{eff}/G_D at PANDA

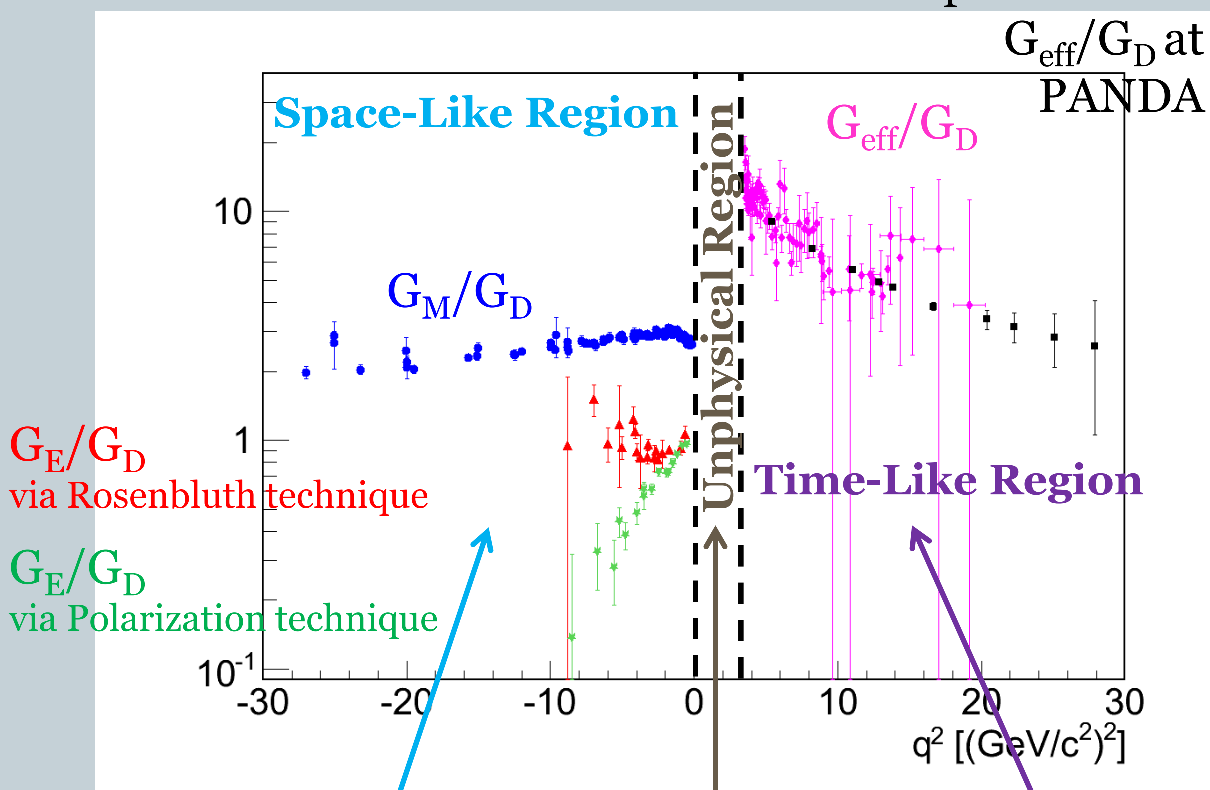

Dispersion relation:

(q²<0)

$$G\left(q^2\right) = \frac{1}{\pi}\left[\int_{4M_\pi^2}^{4M_p^2}\frac{\operatorname{Im}G(s)\,ds}{s-q^2} + \int_{4M_p^2}^{\infty}\frac{\operatorname{Im}G(s)\,ds}{s-q^2}\right]$$

Outline

I. Physics motivations: the proton electromagnetic form factors
II. Model for $\bar{p}p \rightarrow \pi^0 e^+ e^-$
III. Hadronic tensor extraction
IV. Proton electromagnetic form factor extraction
V. Conclusion and outlook

$\bar{p}p \rightarrow \pi^o e^+ e^-$ in the one nucleon exchange model

Differential cross section

$$\frac{d^5\sigma}{dq^2 d\Omega_{\pi^0} d\Omega_e^*} \propto L^{\mu\nu} H_{\mu\nu}\left(s, q^2, \theta_{\pi^0}, G_E, G_M\right)$$

Calculation by J. Van de Wiele

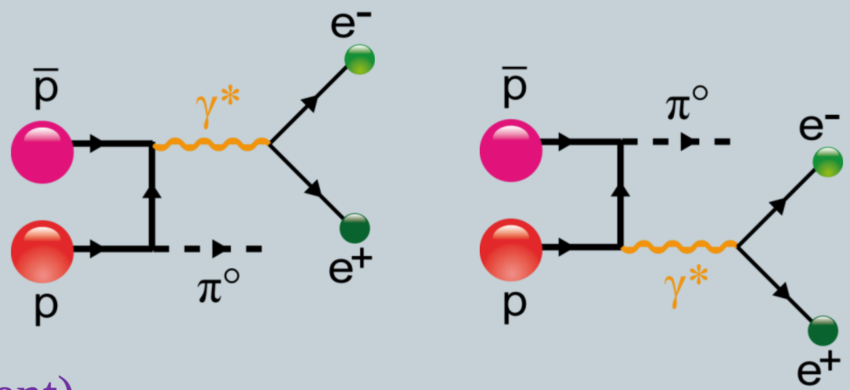

In the γ* rest frame (unpolarized experiment)

$$L^{\mu\nu} H_{\mu\nu} = 4e^2 \frac{q^2}{2}\left(H_{11} + H_{22} + H_{33}\right)$$

$$-8e^2 p_e^{*2}\left(H_{11} \sin^2\theta_e^* \cos^2\varphi_e^* + 2H_{13} \sin\theta_e^* \cos\theta_e^* \cos\varphi_e^*\right.$$

$$\left. + H_{22} \sin^2\theta_e^* \sin^2\varphi_e^* + H_{33} \cos^2\theta_e^*\right)$$

The angular distribution in θ_e^* and φ_e^* gives access to 4 $H_{\mu\nu}$

Constraint by the p̄p→π°γ data

Model constraints

- No data for p̄p→π°e⁺e⁻
- Data for p̄p→π°γ

Differential cross section

$$d^2\sigma \propto |M|^2 \propto g^{\mu\nu} H_{\mu\nu}\left(s, q^2 = 0, \theta_{\pi^0}, G_E(q^2=0), G_M(q^2=0)\right)$$

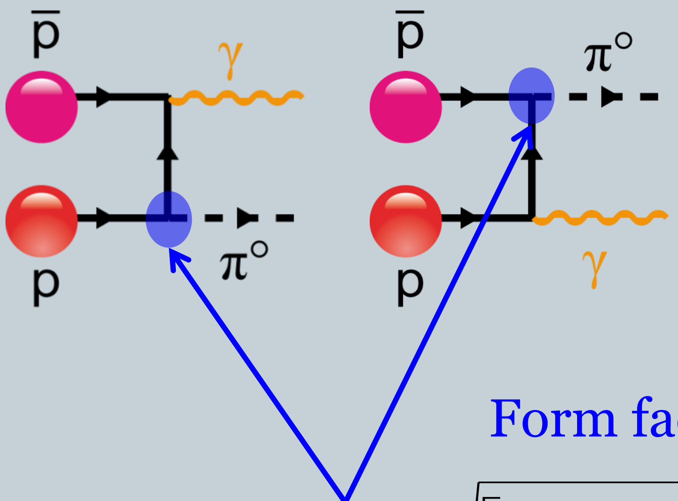

Form factor F:

$$F(\lambda) = \sqrt{\left[\frac{\lambda^2 - M_p^2}{\lambda^2 - p_{X_1}^2}\right]^2 \left[\frac{\lambda^2 - M_p^2}{\lambda^2 - p_{X_2}^2}\right]^2}$$

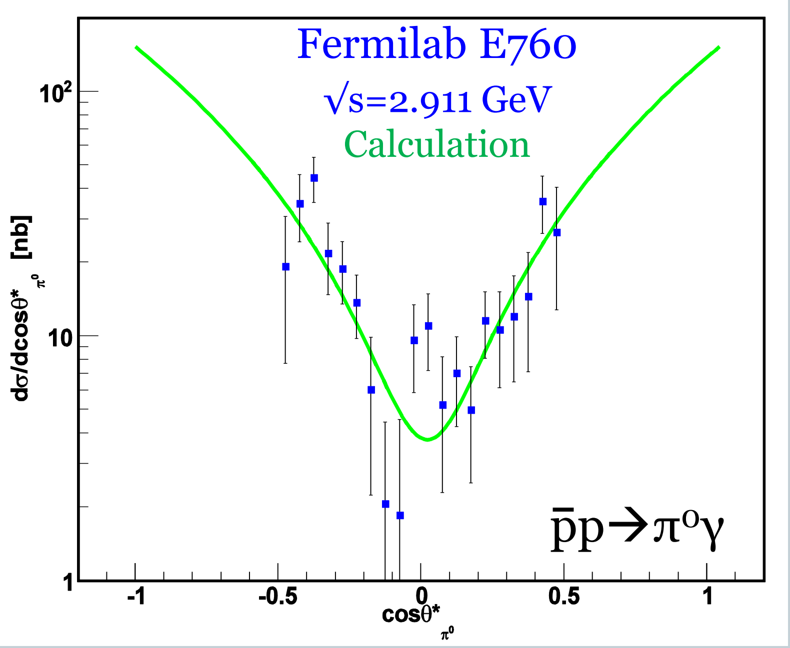

Effect of the F(λ) on the $\bar{p}p \rightarrow \pi^o e^+ e^-$ cross section

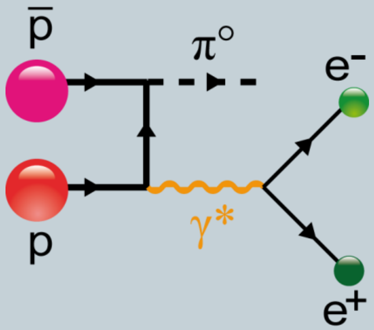

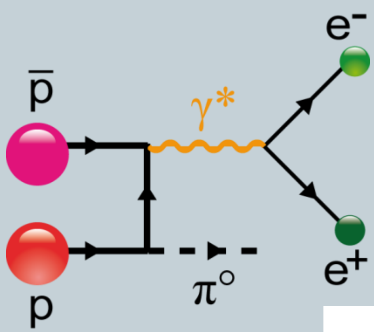

$T_{\bar{p}}$=1. GeV (s=5.4 GeV²)
q^2_{max}=4.8 (GeV/c²)²

At $T_{\bar{p}}$=1. GeV, λ=1.25 GeV/c²

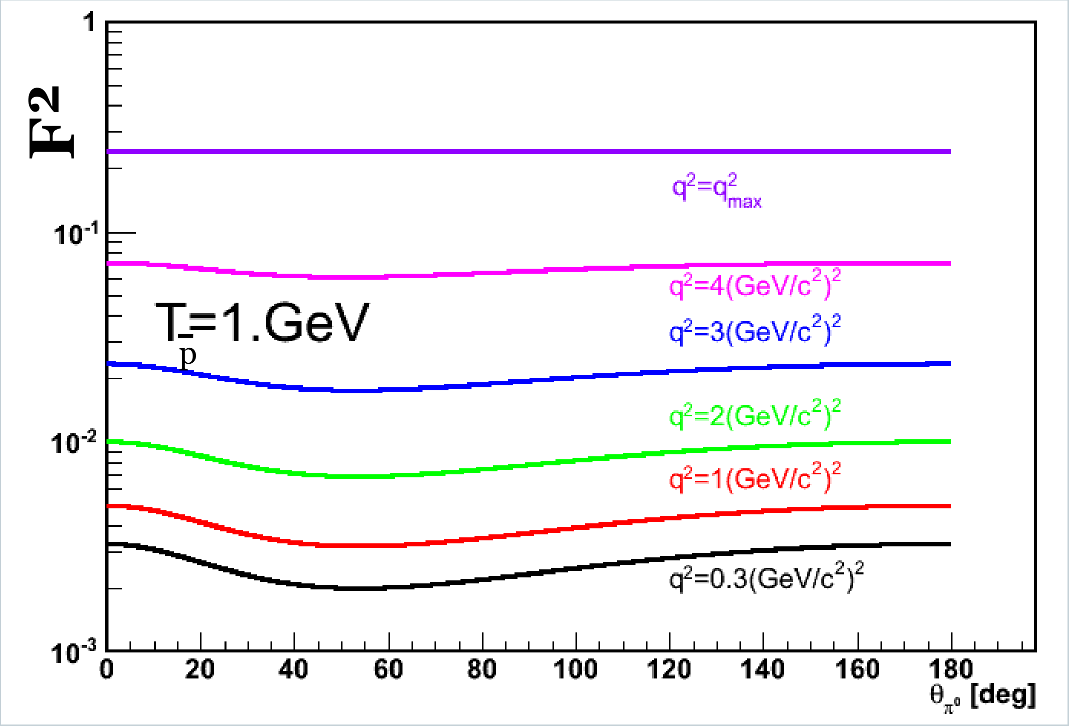

Outline

I. Physics motivations: the proton electromagnetic form factors
II. Model for $\bar{p}p \rightarrow \pi^{0} e^{+} e^{-}$
III. Hadronic tensor extraction
IV. Proton electromagnetic form factor extraction
V. Conclusion and outlook

Choice of the test cases

Vector Meson Dominance (VMD)

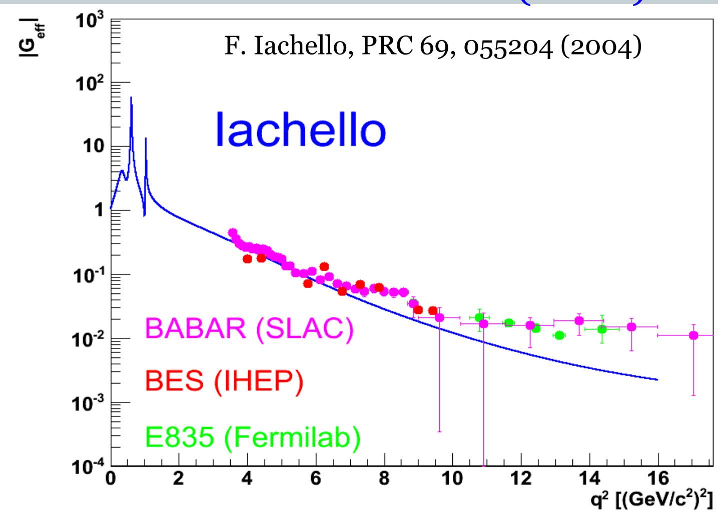

Differential cross section $d\sigma/dq^2$

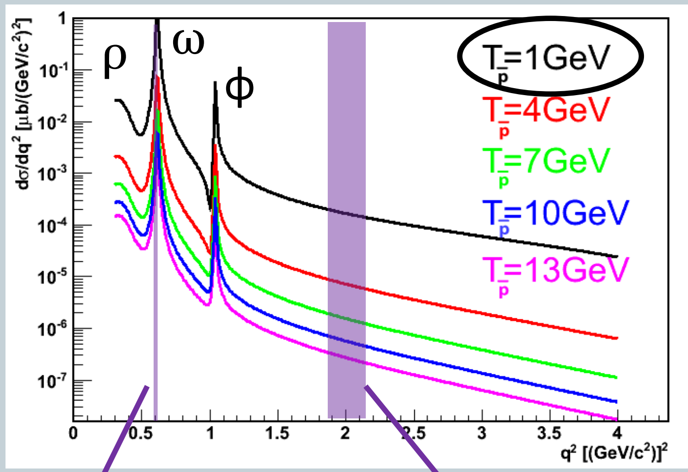

Counting rate ($\Delta\theta_{\pi^0}=1°$)

$$L_{int} = 2\ fb^{-1}$$ (4 month data taking)

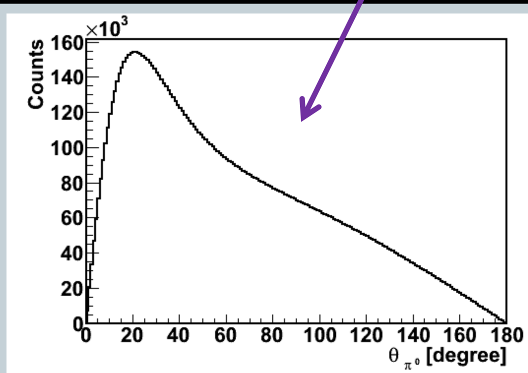

$q^2=0.6\pm0.005$ (GeV/c^2)^2

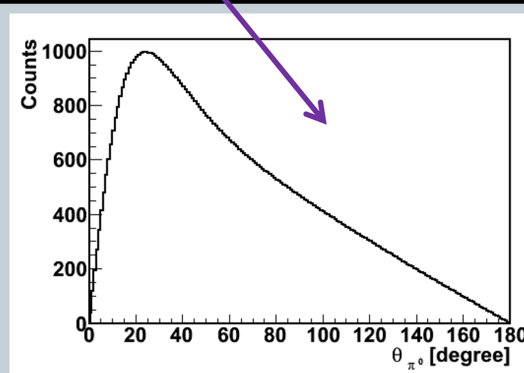

$q^2=2.0\pm0.125$ (GeV/c^2)^2

Hadronic tensor extraction: proof of principle

$L_{\text{int}} = 2\ fb^{-1}$

- $T_{\bar{p}}$=1GeV
- q^2=2.0 ± 0.125 $(GeV/c^2)^2$

For each θ_{π^0} interval ($\Delta\theta_{\pi^0}$=1°):

- $d^2\sigma/d\Omega_e^*$ is generated in the γ^* rest frame (θ_e^*, φ_e^*:10°/bin)
- $d^2\sigma/d\Omega_e^*$ is fitted in the γ^* rest frame taking into account all bins. Monte Carlo method is used to determined the errors.

→experimental determination of $H_{\mu\nu}$

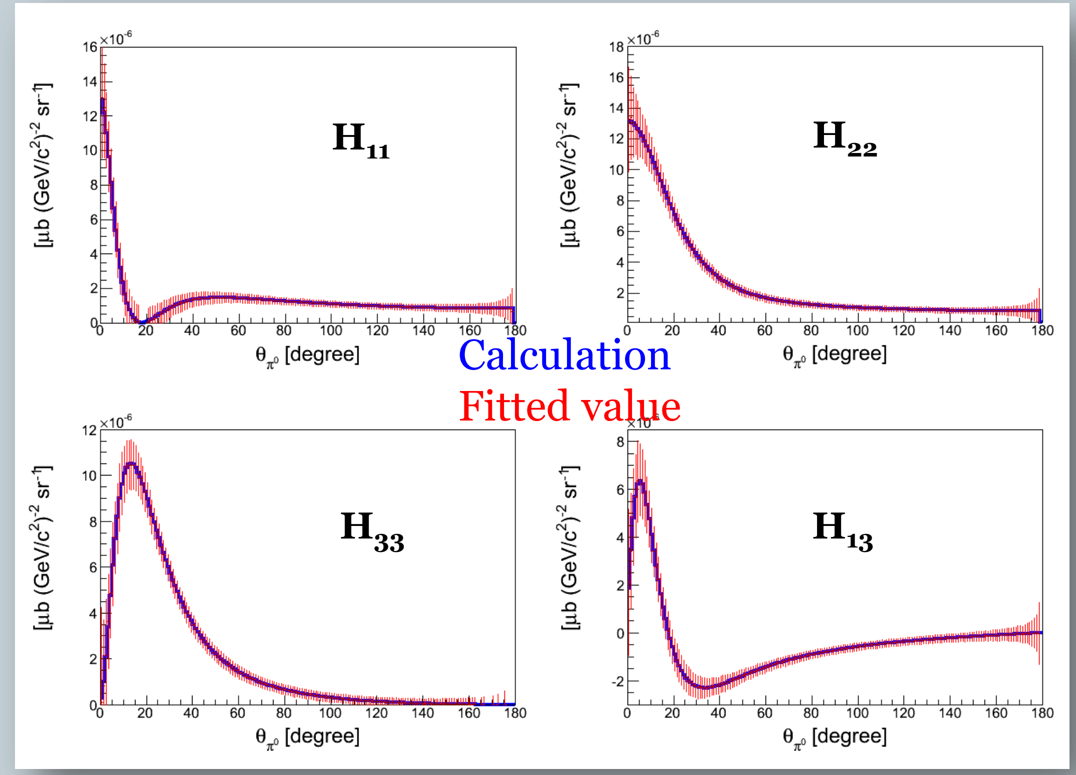

Only statistical errors without acceptance nor efficiency

Direct access to $H_{\mu\nu}$ via the angular distribution valid whatever the model is

Outline

I. Physics motivations: the proton electromagnetic form factors
II. Model for $\bar{p}p \rightarrow \pi^0 e^+ e^-$
III. Hadronic tensor extraction
IV. Proton electromagnetic form factor extraction
V. Conclusion and outlook

From hadronic tensors to form factors

Accessing the proton FFs

$$H_{\mu\nu} = \alpha_{\mu\nu}|G_E|^2 + \beta_{\mu\nu}|G_M|^2 + \gamma_{\mu\nu}|G_E||G_M|\cos(\varphi_E - \varphi_M)$$

↳ $\alpha_{\mu\nu}$, $\beta_{\mu\nu}$ and $\gamma_{\mu\nu}$ depend on s, q^2 and θ_{π^0}.
G_E and G_M only depend on q^2 (on-shell nucleon).

↓

At fixed $T_{\bar{p}}$, q^2, θ_{π^0}, the angular distribution of $\gamma^* \to e^+e^-$ is driven by G_E and G_M.

↓

Without control on the absolute normalization (model), one uses ratios of $H_{\mu\nu}$ and access only two parameters: $R=|G_E|/|G_M|$ and $\cos(\varphi_E-\varphi_M)$.

Choice of the test cases

Differential cross section dσ/dq²

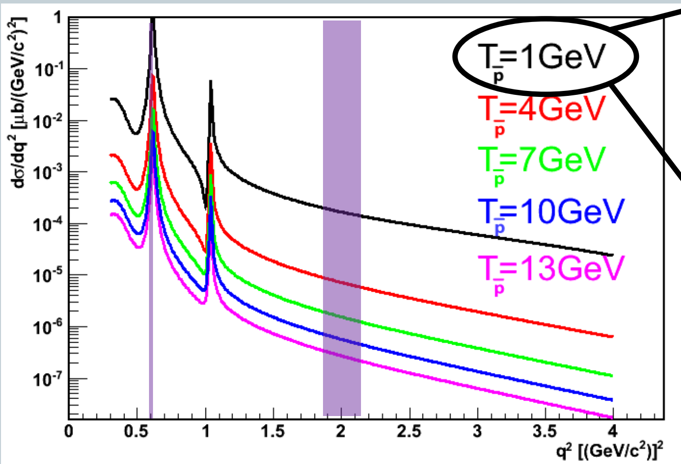

Counting rate ($\Delta\theta_{\pi^\circ}$=1°)

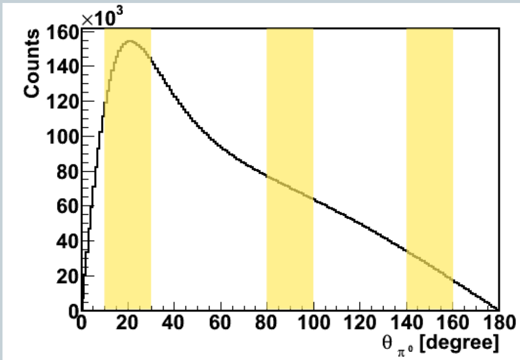

q²=0.6±0.005 (GeV/c²)²

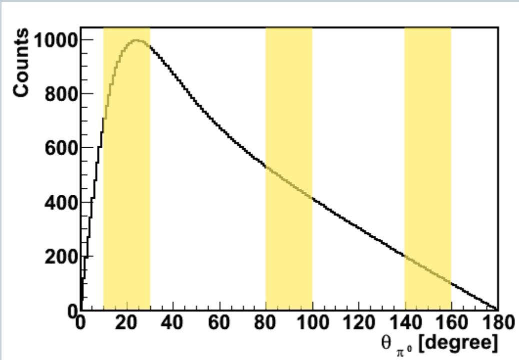

q²=2.0±0.125 (GeV/c²)²

$$L_{\rm int} = 2\, fb^{-1}$$

$T_{\bar{p}}$=1GeV

q²=0.605 ± 0.005 (GeV/c²)²

q²=2 ± 0.125 (GeV/c²)²

$10^\circ < \theta_{\pi^\circ} < 30^\circ$

$80^\circ < \theta_{\pi^\circ} < 100^\circ$

$140^\circ < \theta_{\pi^\circ} < 160^\circ$

Background studies

Background channel rejection:

1. More than 2 charged particles
   → Supression using tracking constraints
2. Two charged particles
   → Dominated by pions
   - Particle Identification (PID) for e/π discrimination
   - Kinematical constraints

$\bar{p}p \rightarrow \pi^+ \pi^- \pi^0$

Bacon et al., PRD 7 (1973)

$T_{\bar{p}}$ [GeV]	σ_{data}[μb]
0.772	1742 ± 71
0.960	1260 ± 70
1.092	1120 ± 70

	σ_{data}[μb]
$\bar{p}p \rightarrow \pi\rho^\pm$	215 ±78
$\bar{p}p \rightarrow \pi^o\rho^o$	251 ±61
$\bar{p}p \rightarrow \pi f_2$	295 ±73

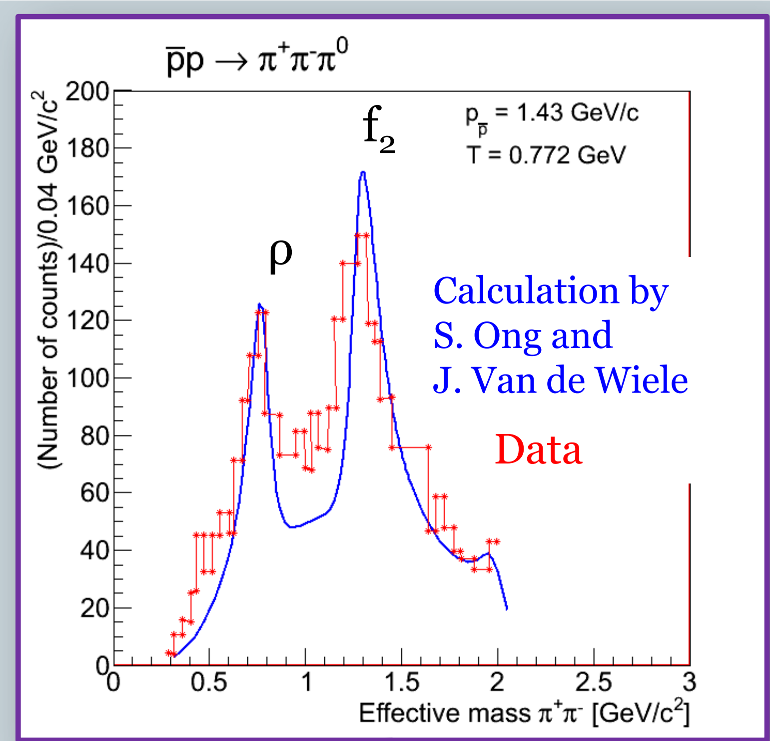

Signal contamination

Signal contamination
To be minimized

Aim: S_c below 1%

Several cut combinations were tested and optimized to minimize $\varepsilon_B/\varepsilon_S$

$$S_c\left(s, q^2, \Omega_{\pi^0}, \Omega_e^*\right) = \frac{\sigma_B}{\sigma_S}\frac{\varepsilon_B}{\varepsilon_S}$$

Background acceptance and efficiency (10^8 events per case)

Signal acceptance and efficiency (10^6 events per case)

Given by models

σ_B/σ_S= a few 10^4 at q^2=0.6 $(GeV/c^2)^2$
σ_B/σ_S= a few 10^6 at q^2=2.0 $(GeV/c^2)^2$

Signal acceptance and efficiency matrix

$\bar{p}p \rightarrow \pi^o e^+ e^-$ at $T_{\bar{p}}$=1 GeV,

q^2=2.0 ± 0.125 $(GeV/c^2)^2$, 10°<θ_{π^o}<30°

10^6 events generated per case

Full event characterization:

1. Two unlike sign charged particles (c^+,c^-)
2. Reconstruction of a π^o
   a. Two photons (γ_1,γ_2) of at least 30 MeV each
   b. 0.115<Invariant mass (γ_1,γ_2)<0.150 GeV/c^2
3. Particle identification combined likelihood (truncated dE/dx, ECAL, Cherenkov angle)
   a. c^+ is e^+ with a probability larger than 99.8%
   b. c^- is e^- with a probability larger than 99.8%
4. Kinematical constraints

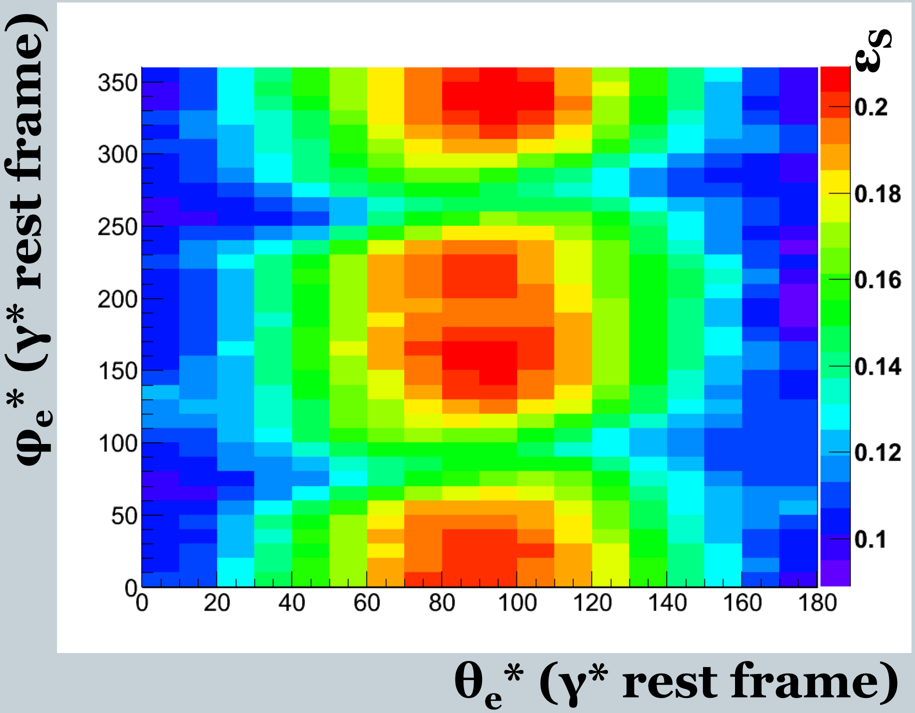

From theoretical to experimental distribution

$L_{int} = 2\ fb^{-1}$

$T_{\bar{p}}$=1GeV, q^2=2.0 ± 0.125 $(GeV/c^2)^2$, $10° < \theta_{\pi°} < 30°$

N^{th}_{ij} (model)

Effect of acceptance and efficiency →

μ^{th}_{ij}

← Poisson distribution

N^{exp}_{ij} (experiment)

Correction for acceptance and efficiency →

N^{cor}_{ij}

$|G_E|/|G_M|$ and $\cos(\varphi_E-\varphi_M)$

Monte Carlo x 2000

Error estimates

N^{th}=18 486

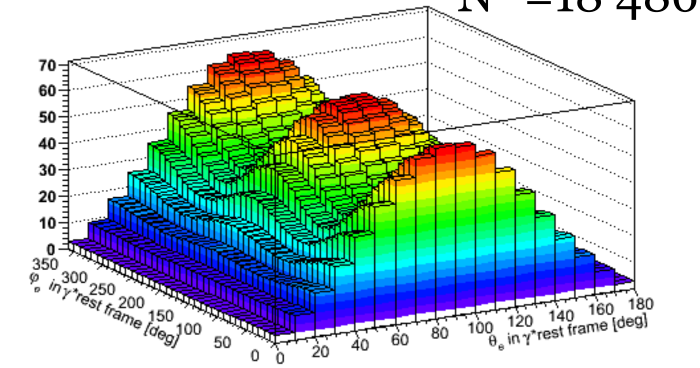

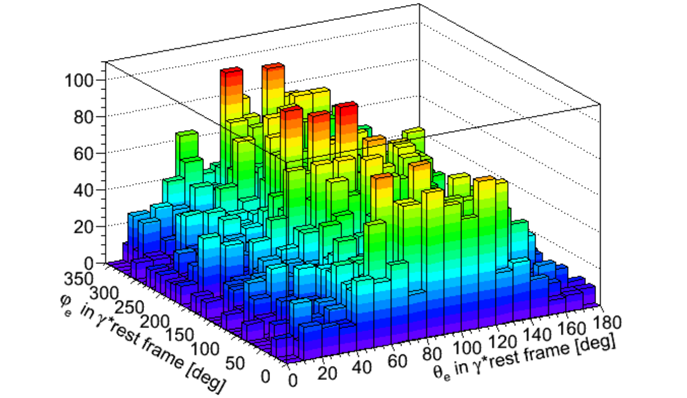

From theoretical to experimental distribution

$T_{\bar{p}}$=1GeV, q^2=2.0 ± 0.125 $(GeV/c^2)^2$ $L_{int} = 2\ fb^{-1}$

Theoretical distributions

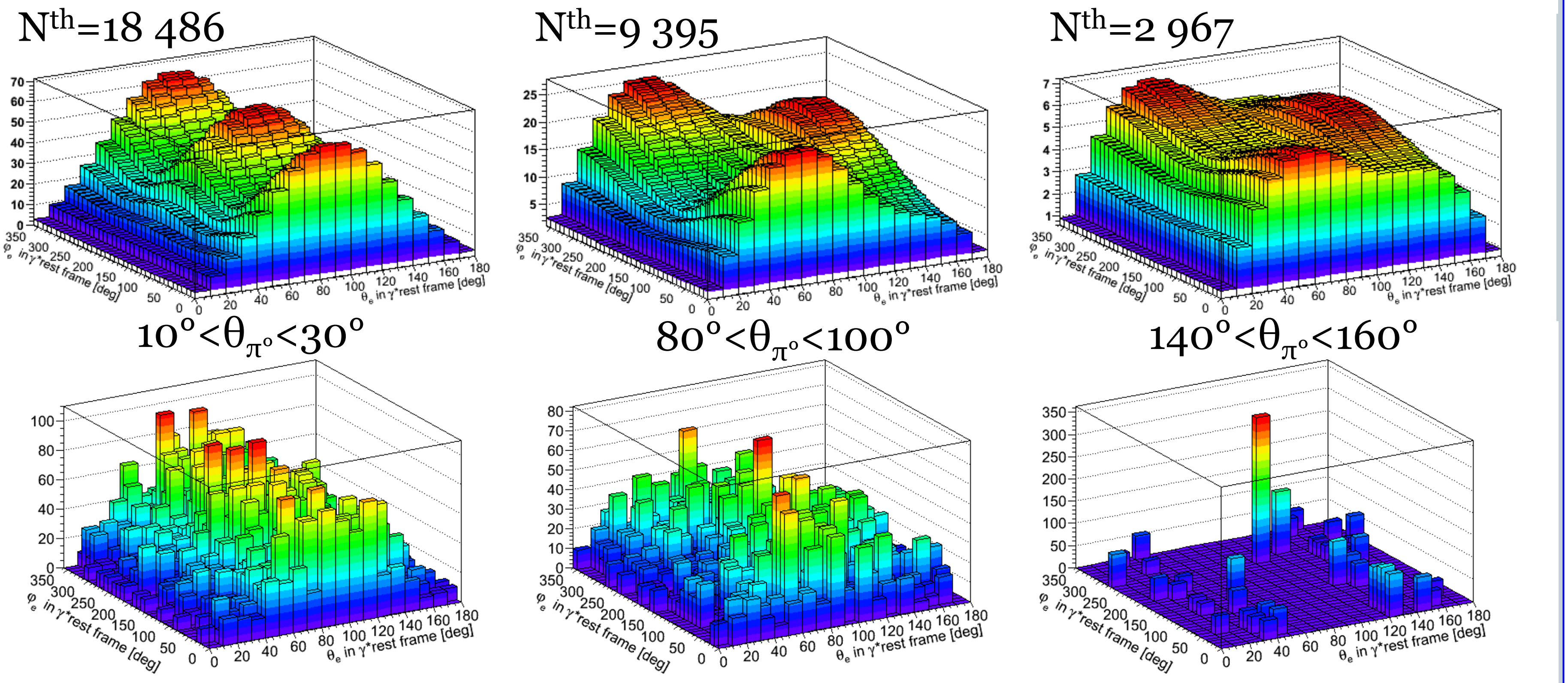

Experimental distributions corrected for acceptance and efficiency

From experimental to physical information

$T_{\bar{p}}$=1GeV, q^2=2.0 ± 0.125 $(GeV/c^2)^2$

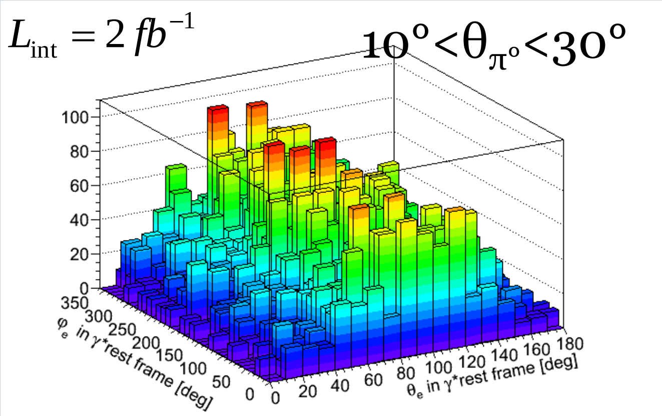

Corrected experimental distribution

Projections:

Avoid fitting problems due to low statistics. Extraction of 3 independent asymmetry parameters

↓

Information on the form factors

$$\int_0^{2\pi} N(\Omega_e^*)\, d\varphi_e^*$$

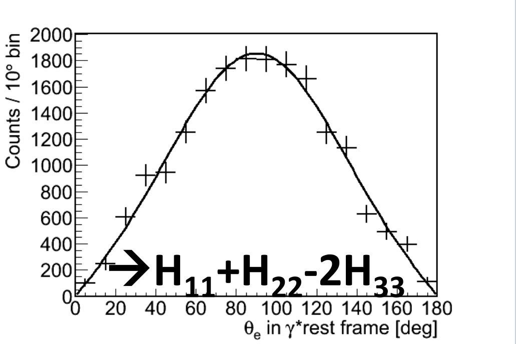

$$\int_{-1}^{1} N(\Omega_e^*)\, d\cos\theta_e^*$$

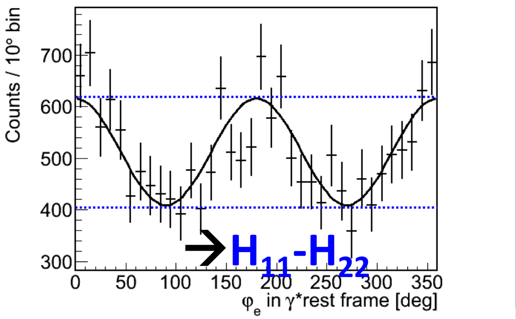

$$\int_0^{1} N(\Omega_e^*)\, d\cos\theta_e^*$$

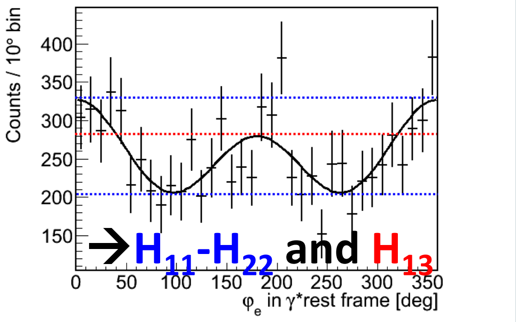

Error estimates

$T_{\bar{p}}$=1GeV, q^2=2.0 ± 0.125 $(GeV/c^2)^2$,
$10° < \theta_{\pi°} < 30°$

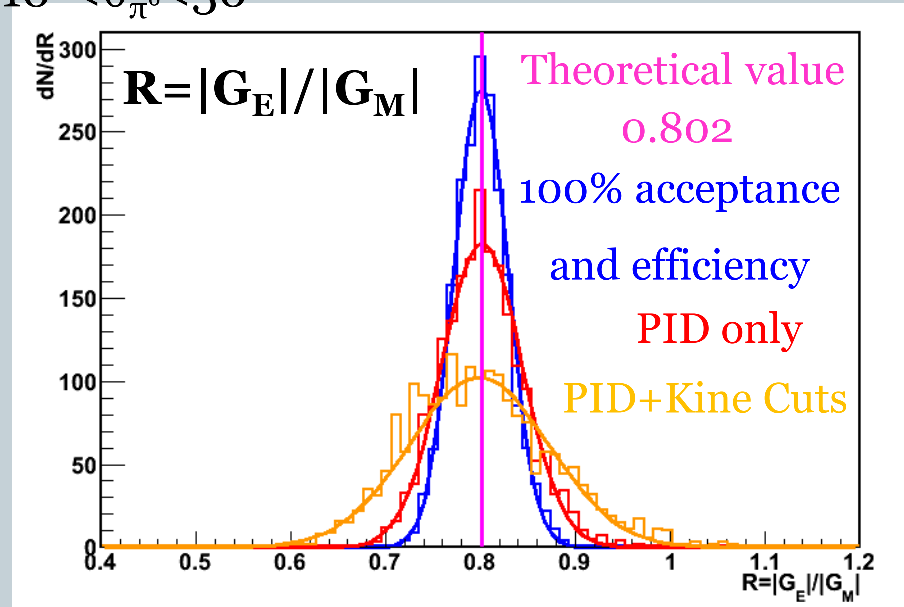

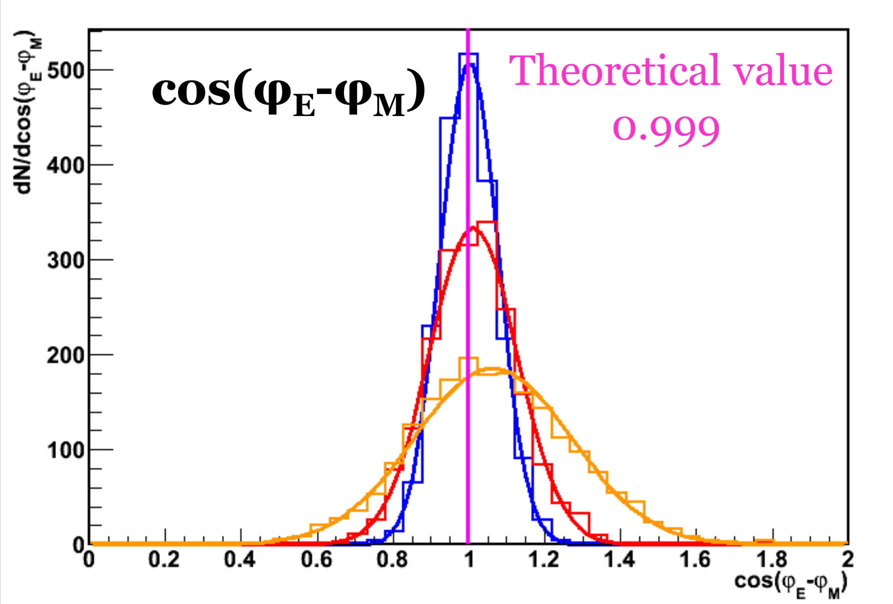

Form factor ratio R can be extracted

For the first time $\cos(\varphi_E-\varphi_M)$ can be extracted

$L_{\text{int}} = 2\, fb^{-1}$

Expected precision

$q^2 = 0.605 \pm 0.005\ (GeV/c^2)^2$ $q^2 = 2.0 \pm 0.125\ (GeV/c^2)^2$

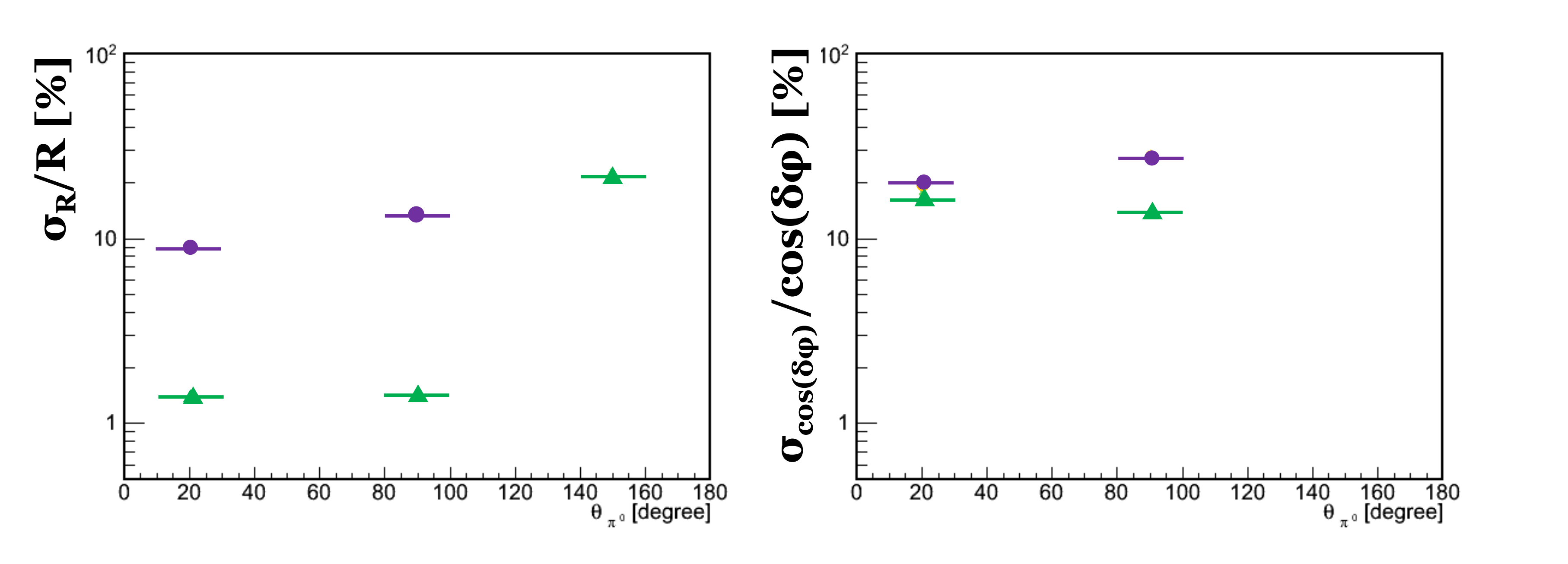

Form factor ratio R can be extracted close to the ω resonance with 1% precision and at q^2 close to 2 $(GeV/c^2)^2$ with 10% precision

For the first time $\cos(\varphi_E - \varphi_M)$ can be extracted with 10-30% precision

$$L_{\text{int}} = 2\ fb^{-1}$$

Conclusion

- $\bar{p}p \to \pi^0 e^+ e^-$ was proposed to access the proton FFs in the unphysical region.

- A model for $\bar{p}p \to \pi^0 e^+ e^-$ was developed and constrained by $\bar{p}p \to \pi^0 \gamma$ data.
- Access to the hadronic tensors $H_{\mu\nu}$ is possible via the lepton angular distribution.
- Access to $R=|G_E|/|G_M|$ and $\cos(\varphi_E-\varphi_M)$ via the lepton angular distribution.

- Background studies:
  - Model for background to signal cross section ratio
  - Background supression studies useful for other models (s-channel, Δ or N* in t-channel, TDA, …)
  - Determination of signal contamination

- $R=|G_E|/|G_M|$ and $\cos(\varphi_E-\varphi_M)$ are extracted and the precision is estimated via a Monte Carlo method.

Outlook

• Measurement of the angular distribution of the $\bar{p}p \rightarrow \pi^o\gamma$ channel to constrain better the model.

• Measurement of angular distribution of the $\bar{p}p \rightarrow \pi^o\pi^+\pi^-$ channel over the whole phase space.

• Angular distribution of the $\bar{p}p \rightarrow \pi^o e^+e^-$ channel
  - Is the one nucleon exchange diagram dominant?
  - Comparison of R from $\bar{p}p \rightarrow \pi^o e^+e^-$ and $\bar{p}p \rightarrow e^+e^-$ for $q^2>4M_p^2$
  - Dependence of the extracted R and $\cos(\varphi_E-\varphi_M)$ on θ_{π^o}, s, ...

Merci!

Transition Distribution Amplitude approach

J.P. Lansberg, B. Pire an L. Szymanowski
PRD 76, 111502 (2007)

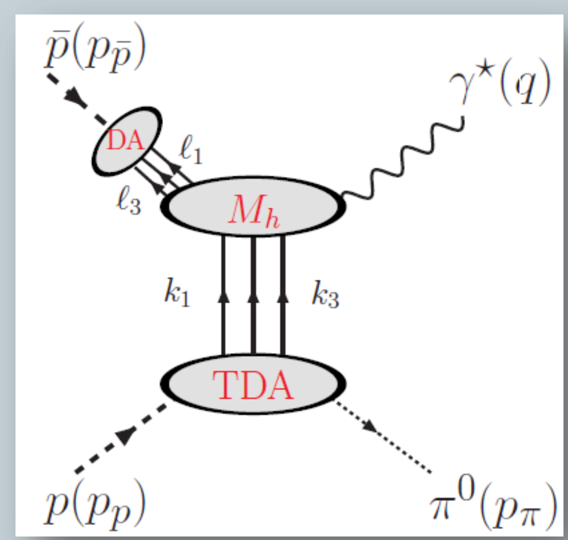

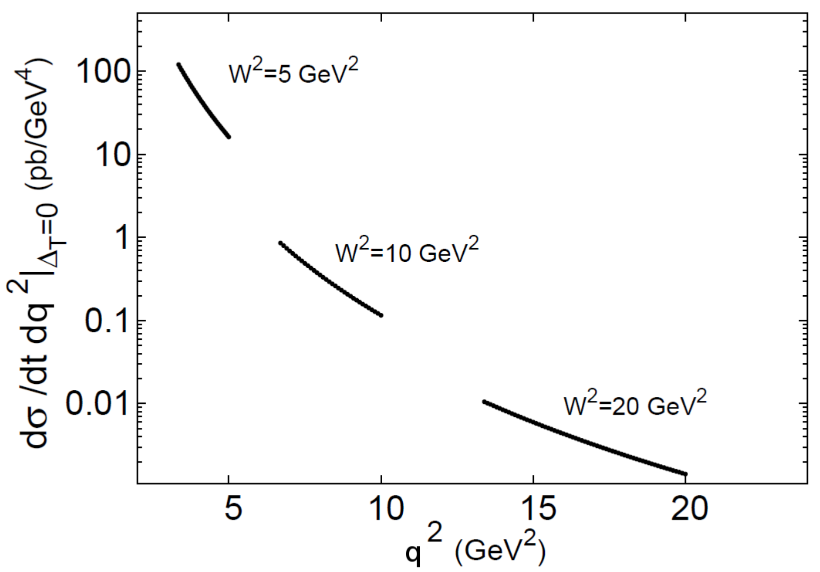

Validity:

- q^2 of the order of s
- Small t or small u

→ Not suited for the study of the proton form factors far below threshold ($q^2 \ll M_p^2$)

Time-Like form factor parametrizations

Vector Meson Dominance (VMD)

F. Iachello, PRC 69, 055204 (2004)

Meson poles. ρ, ω and ϕ resonances

« pQCD inspired »

$$|G_E| = |G_M| = \frac{const\ GeV^4}{q^4\left(\ln^2\frac{q^2}{\Lambda^2}+\pi^2\right)}$$

$$q^2 > \Lambda^2 = 0.3^2 (GeV/c)^2$$

S. J. Brodsky and G. R. Farrar, PRL 31, 1153 (1973)

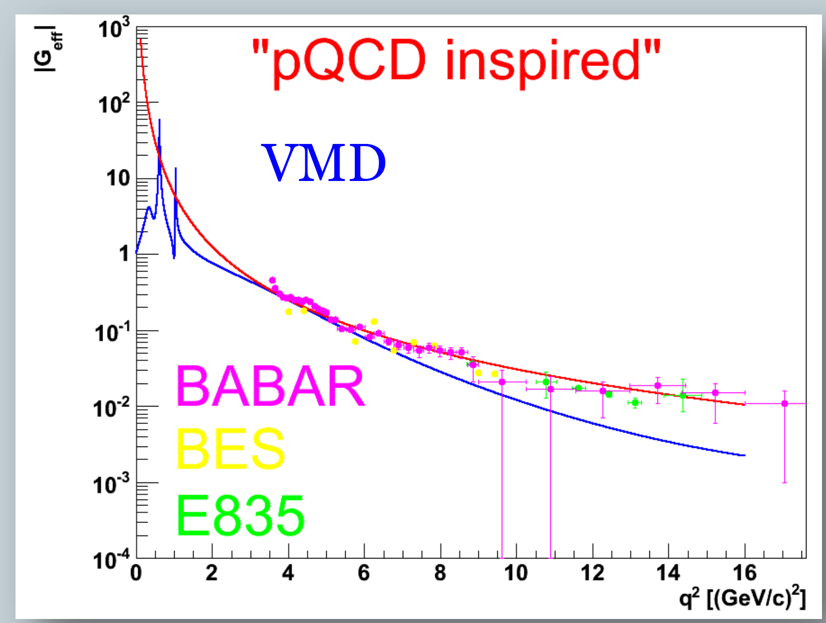

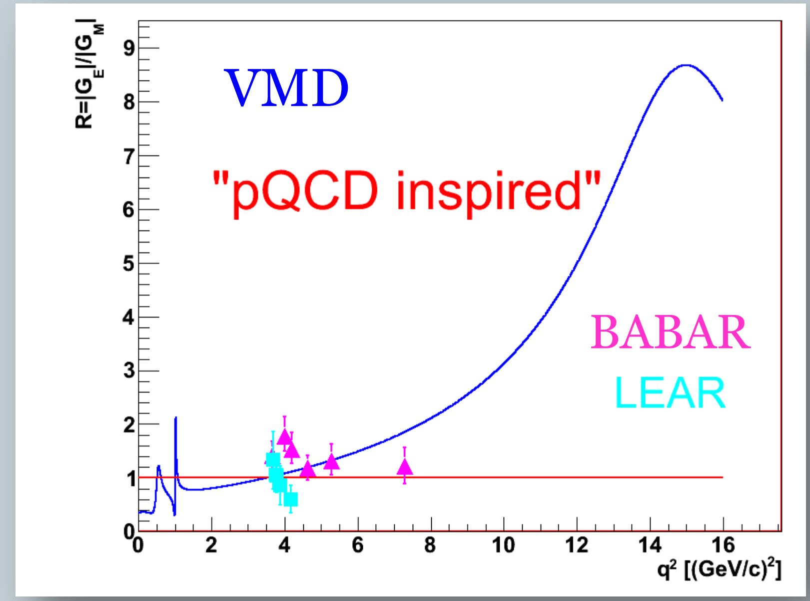

One Nucleon Exchange model

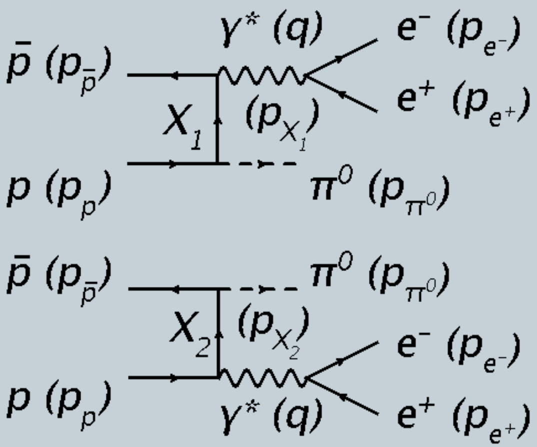

C. Adamuščín, PRC 75, 045205 (2007)

$$\frac{d^2\sigma}{dq^2\,d\cos\theta_{\pi^0}} \propto \frac{\alpha^2}{6s\pi}\frac{\beta_e}{\beta_p} D \frac{M_p^2}{s^2(1-\beta_p\cos\theta_{\pi^0})^2}$$

Contains the FFs

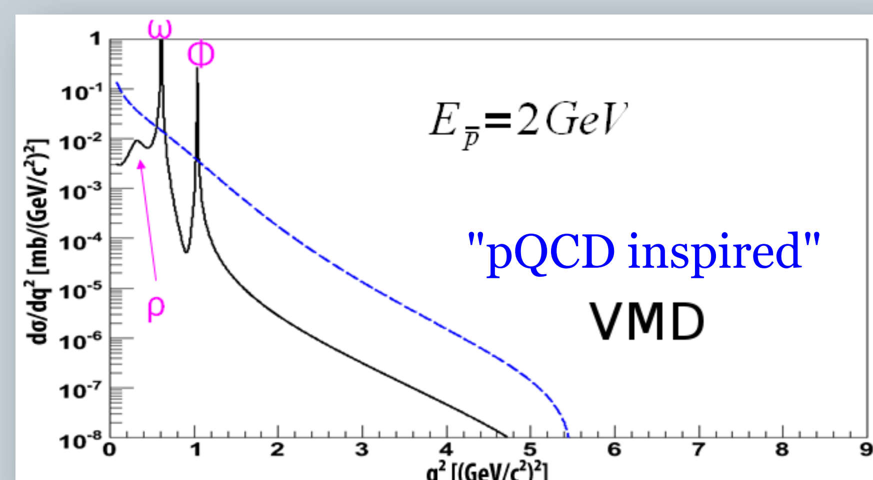

$d^5\sigma$ not available → Not suited for the simulation of the 3-body final states

Model not constrained by data!

Effects of detector resolution

$\bar{p}p \rightarrow e^+e^-\pi^0$ @ $T_{\bar{p}} = 1$ GeV (Phase Space)
within BABAR framework

Full event reconstruction

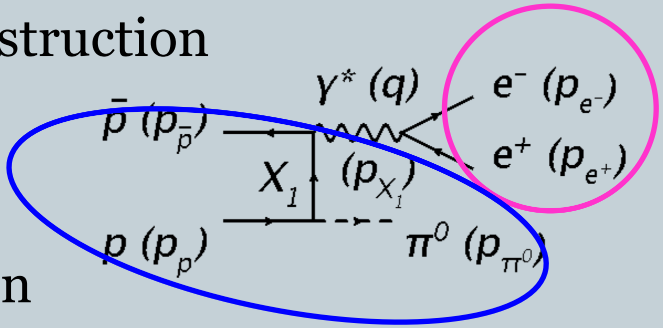

q² reconstruction

- Using e⁺ and e⁻ ➔ $q^2 = |\mathbf{p}_{e+} + \mathbf{p}_{e-}|^2$
- Using π⁰ (2γ) ➔ $q^2 = |\mathbf{p}_{\bar{p}} + \mathbf{p}_p - \mathbf{p}_{\pi 0}|^2$

q² resolution

- Better resolution using e⁺ and e⁻
- Weak dependence on π⁰ angle
- Better results after kinematic fit
- Limited possibility to scan ω resonance

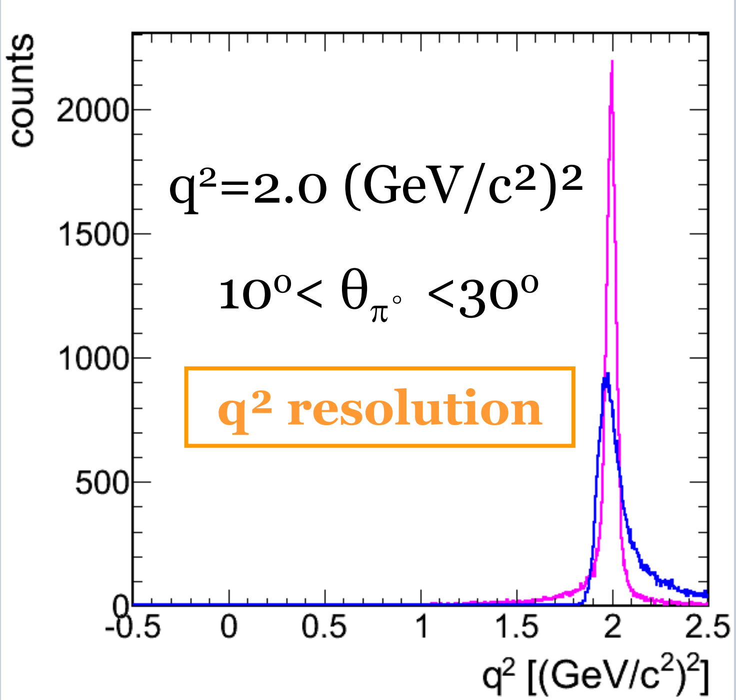

q² (GeV/c²)²	ΔM² (GeV/c²)²	ΔM² (GeV/c²)² After kinemtic fit
0.6	0.023	0.012
2.0	0.063	0.021

$\Delta M_\omega^2 = 0.022$ (GeV/c²)²

In collaboration with T. Liu, M. Gumberidze

The proton composite structure

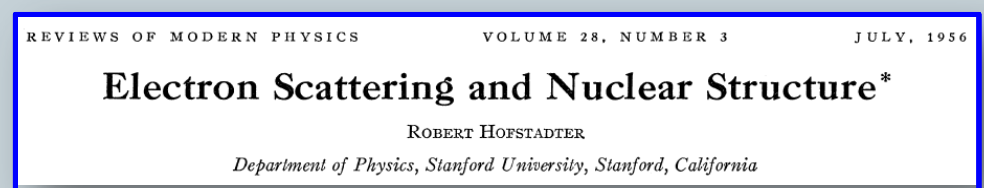

REVIEWS OF MODERN PHYSICS VOLUME 28, NUMBER 3 JULY, 1956

Electron Scattering and Nuclear Structure*

ROBERT HOFSTADTER

Department of Physics, Stanford University, Stanford, California

1. The proton is not point-like,
2. Form factors (FFs) are introduced to describe the elastic scattering.

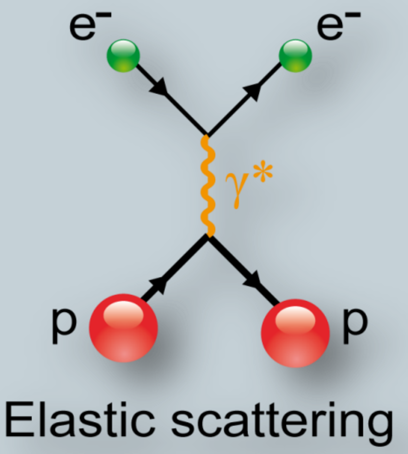

- The proton (S=1/2) has 2S+1 FFs: the electric G_E and the magnetic G_M FFs.
- G_E and G_M are analytical function of one kinematical variable: the 4-momentum transfered squared (q^2) of the virtual photon.
- Schematically:
  - at low energy, they are interpreted in terms of charge and magnetization distributions,
  - at high energy, they test the pQCD predictions

Accessing the proton electromagnetic FFs

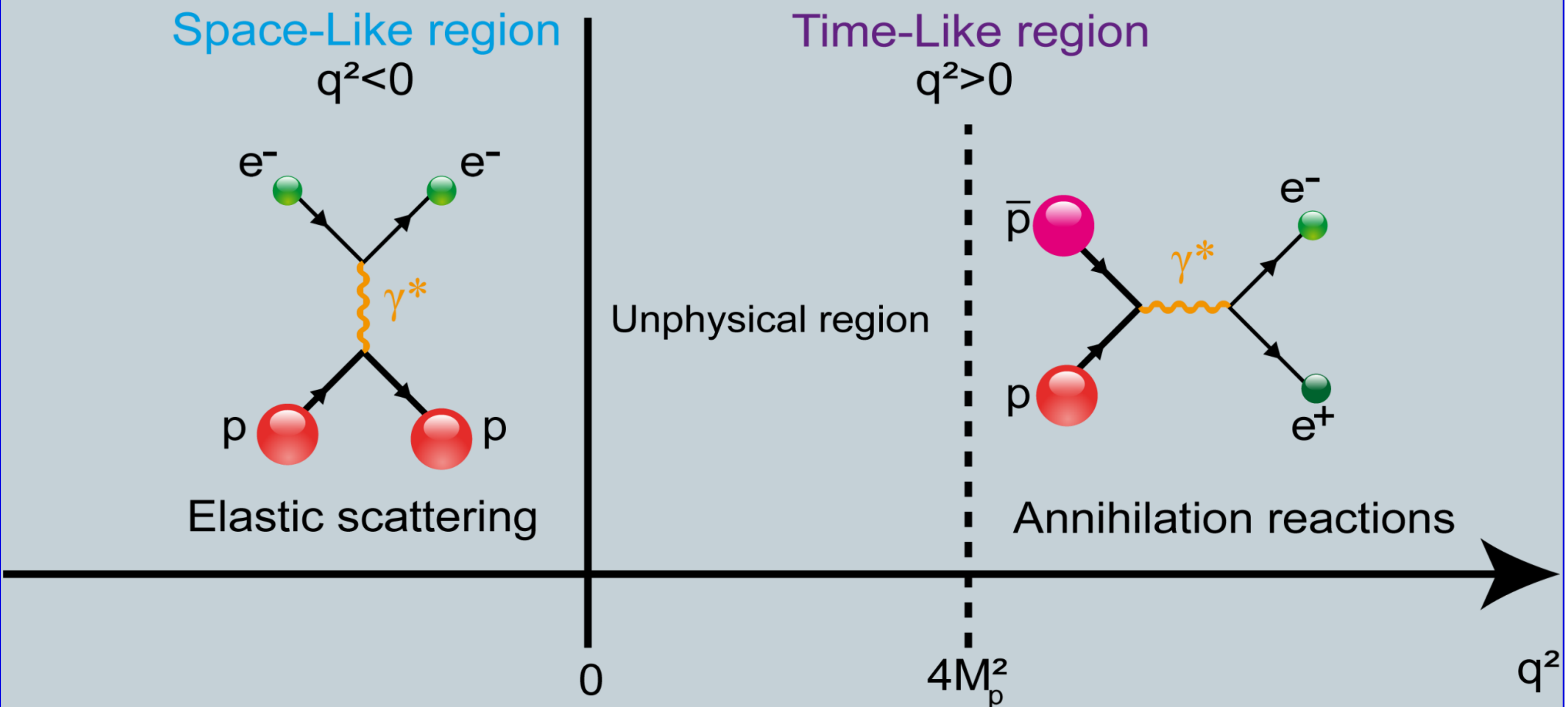

Space-Like region

In the Space-Like region,
G_E and G_M are real functions of q^2.

1. Rosenbluth technique

$$\left(\frac{d\sigma}{d\cos\theta_{e'}}\right)_{lab} = \left(\frac{d\sigma}{d\cos\theta_{e'}}\right)_{Mott} \frac{\tau}{\varepsilon(1+\tau)}\left(G_M^2 + \frac{\varepsilon}{\tau} G_E^2\right)$$

$$\tau = -\frac{q^2}{4M_p^2}, \quad \varepsilon^{-1} = 1 + 2(1+\tau)\tan^2(\theta_{e'}/2)$$

2. Polarization technique

$$R = \frac{G_E}{G_M} = -\frac{P_t}{P_l}\frac{E_e + E_{e'}}{2M_p}\tan(\theta_{e'}/2)$$

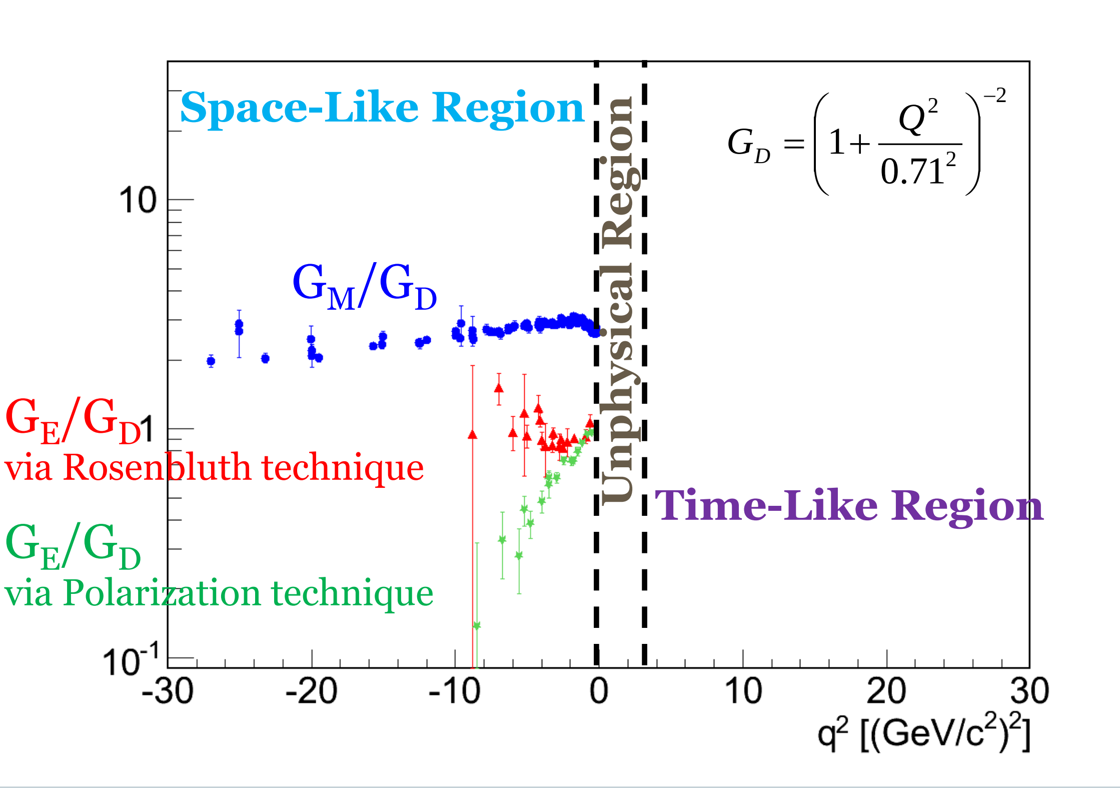

Time-Like region

1. From the differential cross section

$$\left(\frac{d\sigma}{d\cos\theta_e}\right)_{cm} = \frac{\pi(\alpha\hbar c)^2}{8M_p^2\sqrt{\tau(\tau-1)}}\left(\left|G_M\right|^2\left(1+\cos^2\theta_e\right)+\frac{\left|G_E\right|^2}{\tau}\sin^2\theta_e\right)$$

$$\tau = \frac{q^2}{4M_p^2}$$

2. From the total cross section

$$\sigma_{tot} = \frac{\pi(\alpha\hbar c)^2}{6M_p^2}\frac{(2\tau+1)\left|G_{eff}\right|^2}{\tau\sqrt{\tau(\tau-1)}}$$

$$\left|G_{eff}\right|^2 = \frac{2\tau\left|G_M\right|^2+\left|G_E\right|^2}{2\tau+1}$$

In the Time-Like region, G_E and G_M are complex functions of q^2.

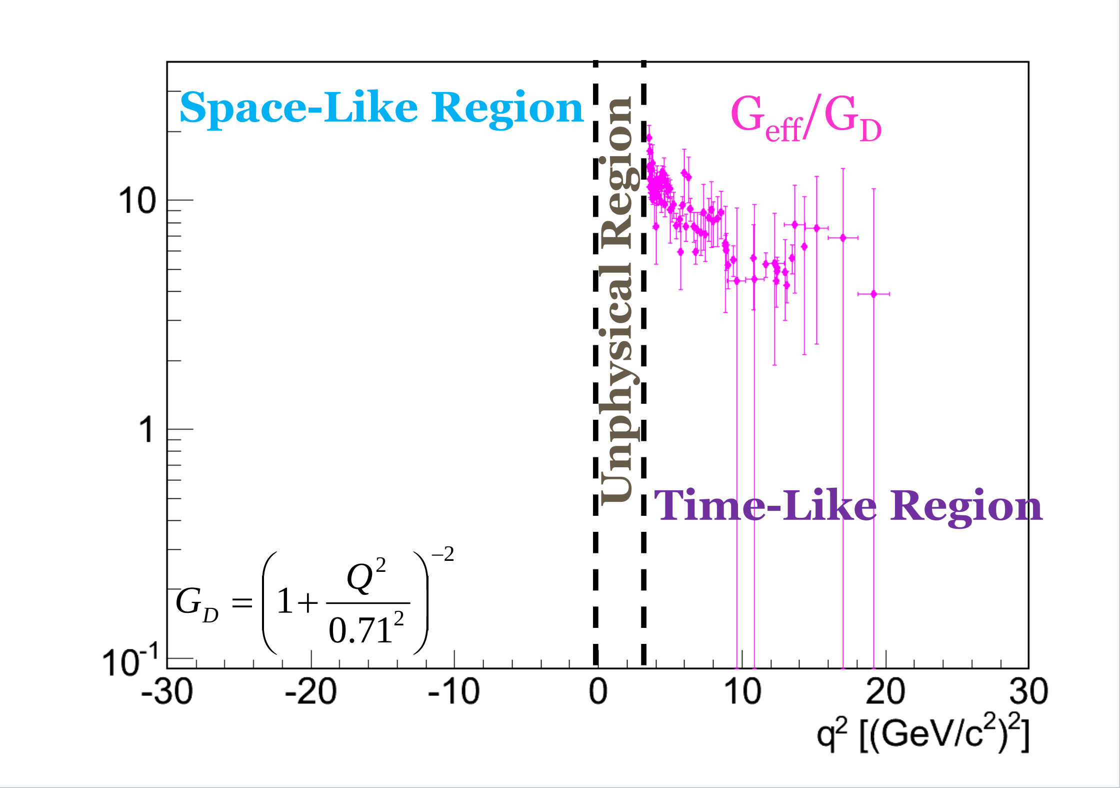

Proton electromagnetic FFs world data

Phragmén-Lindelhöf theorem:

$$\lim_{q^2\to-\infty} G_{E,M}(q^2) = \lim_{q^2\to+\infty} G_{E,M}(q^2)$$

Asymptotics:

$$\lim_{q^2\to\pm\infty} \left|G_{E,M}^{SL,TL}(q^2)\right| = (q^2)^{-2}$$

$G_E(4M_p^2)=G_M(4M_p^2)$

$G_E(0)=1$

$G_M(0)=\mu^p/\mu^N$

Sudoł et al., EPJA 44, 473-384 (2010)

Expected precision on G_{eff}/G_D at PANDA

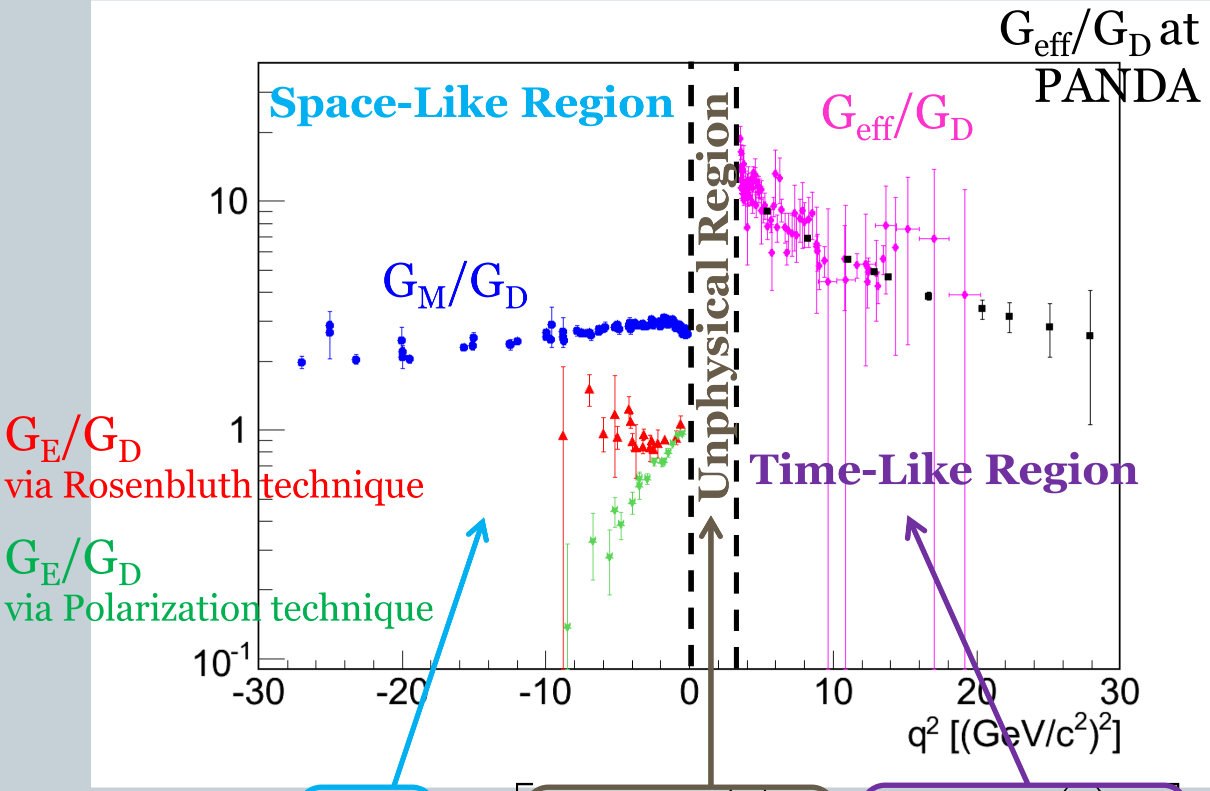

Dispersion relation:
($q^2<0$)

$$G(q^2) = \frac{1}{\pi}\left[\int_{4M_\pi^2}^{4M_p^2} \frac{\operatorname{Im} G(s)\,ds}{s-q^2} + \int_{4M_p^2}^{\infty} \frac{\operatorname{Im} G(s)\,ds}{s-q^2}\right]$$

My PhD thesis

1. Demonstrate the feasibility of the proton electromagnetic form factor measurements in the unphysical region using the $\bar{p}p \rightarrow \pi^0 e^+ e^-$ reaction (original idea by M. P. Rekalo, Sov. J. Nucl. Phys. 1, 1965)

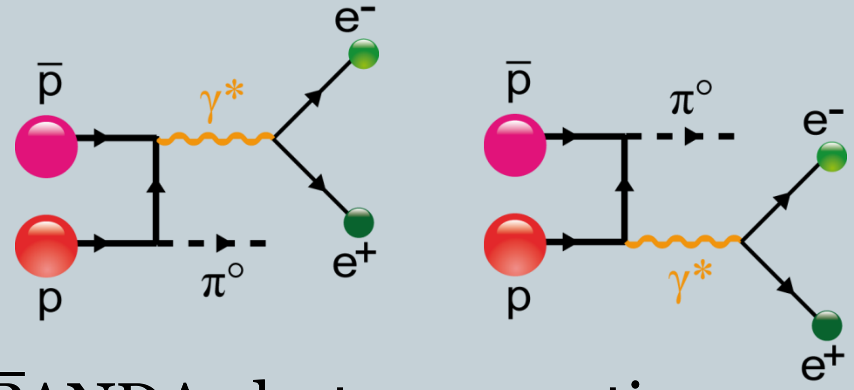

2. Test the prototype of the $\overline{\text{P}}$ANDA electromagnetic calorimeter.

Case $\bar{p}p \rightarrow e^+e^-$

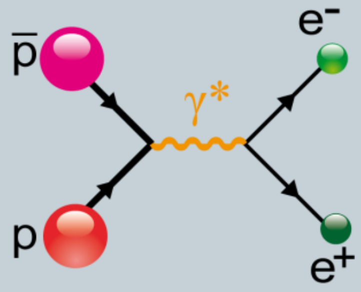

In the γ^* rest frame (equivalent to $\bar{p}p$ CM)

$$L^{\mu\nu}H_{\mu\nu} = 4e^2\frac{q^2}{2}\left(2H_{11}+H_{33}\right)$$

$$-8e^2 p_e^{*2}\left(H_{11}\sin^2\theta_e^* + H_{33}\cos^2\theta_e^*\right)$$

$$\left(\frac{d\sigma}{d\cos\theta_e}\right)_{cm} = \frac{\pi(\alpha\hbar c)^2}{8M_p^2\sqrt{\tau(\tau-1)}}\left(\left|G_M\right|^2\left(1+\cos^2\theta_e\right)+\frac{\left|G_E\right|^2}{\tau}\sin^2\theta_e\right)$$

Feasibility studies of the time-like proton electromagnetic form factor measurements with PANDA at FAIR

Sudoł et al., EPJA 44, 473-384 (2010)

1. Access to $|G_E|$ and $|G_M|$ via the lepton angular distribution
2. Sensitivity to $|G_E|$ and $|G_M|$
3. Background studies
4. Expected precision

Outline

I. Physics motivations: the proton electromagnetic form factors

II. The $\overline{\text{P}}$ANDA detector at FAIR
  1. Facility for Antiproton and Ion Research
  2. antiProton ANnihilation at Darmstadt
  3. Electromagnetic calorimeter prototype

III. Formalism

IV. Feasibility studies of the proton electromagnetic form factor measurements using the $\bar{p}p \rightarrow \pi^0 e^+ e^-$ reaction
  1. Model for $\bar{p}p \rightarrow \pi^0 e^+ e^-$
  2. Hadronic tensor extraction
  3. Proton electromagnetic form factor extraction
     - Choice of the test cases
     - Background studies
     - Expected precision

V. Conclusion and outlook

Facility for Antiproton and Ion Research FAIR

CBM
- Compressed Bayonic Matter
- Nuclear matter physics

NuSTAR
- Nuclear Structure, Astrophysics and Reactions
- Rare isotope beams

APPA
- Atomic, Plasma Physics and Applications
- Heavy ion beams

FLAIR
- Facility for Low energy Antiproton and Ion Research

$\bar{\text{P}}$ANDA
- **antiProton Annihilation at Darmstadt**
- **Hadron and nuclear physics**
- **Antiproton beams**

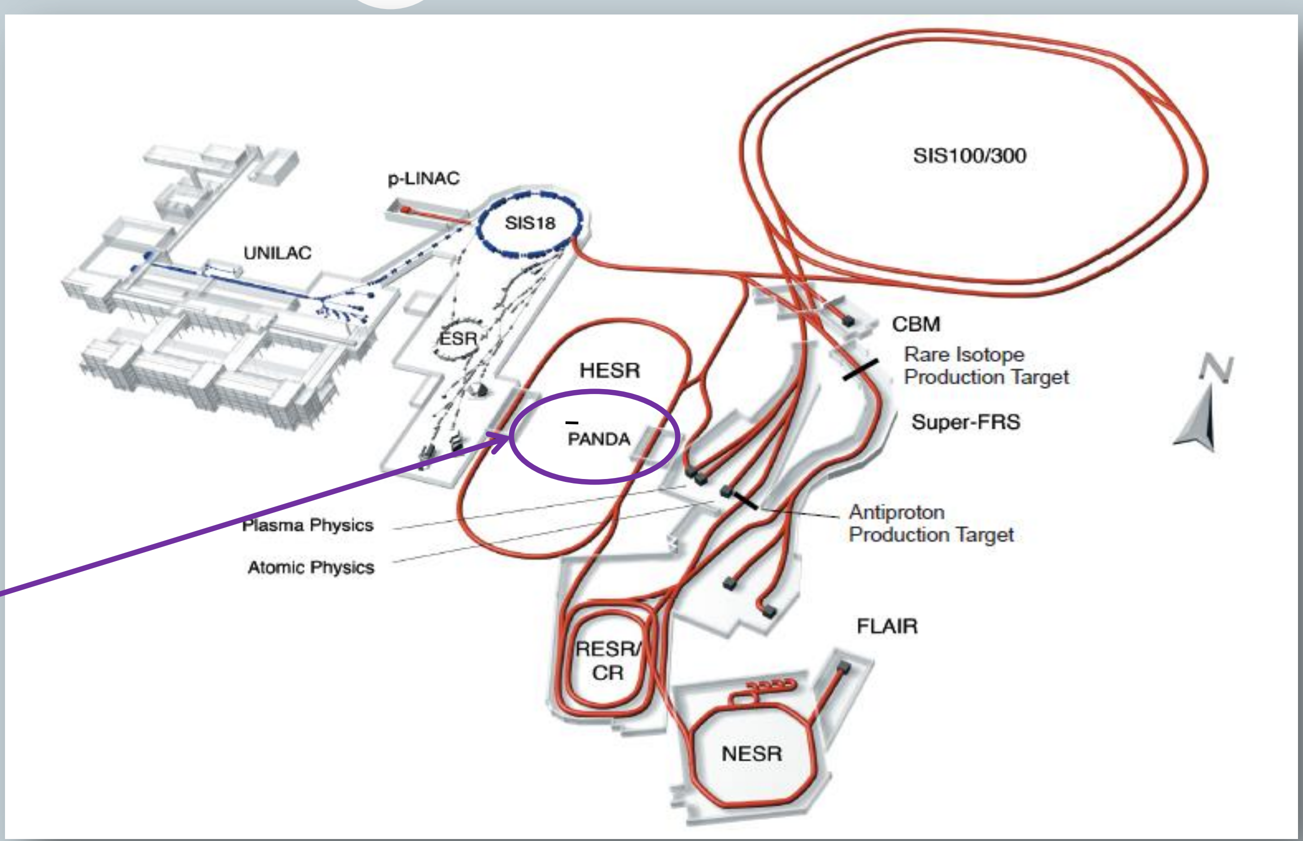

$\bar{p}$ momentum from 1.5 to 15 GeV/c,
luminosity up to 2 10^{32} $cm^{-2}s^{-1}$
First experiment expected around 2019

The $\bar{P}$ANDA experiment

Physics at $\bar{P}$ANDA

- QCD bound states
- Non perturbative QCD dynamics
- Hadrons in nuclear matter
- Hypernuclear physics
- Electroweak physics
- Electromagnetic processes

$\bar{P}$ANDA collaboration

- 450 scientists
- 17 countries

IPN Orsay contribution

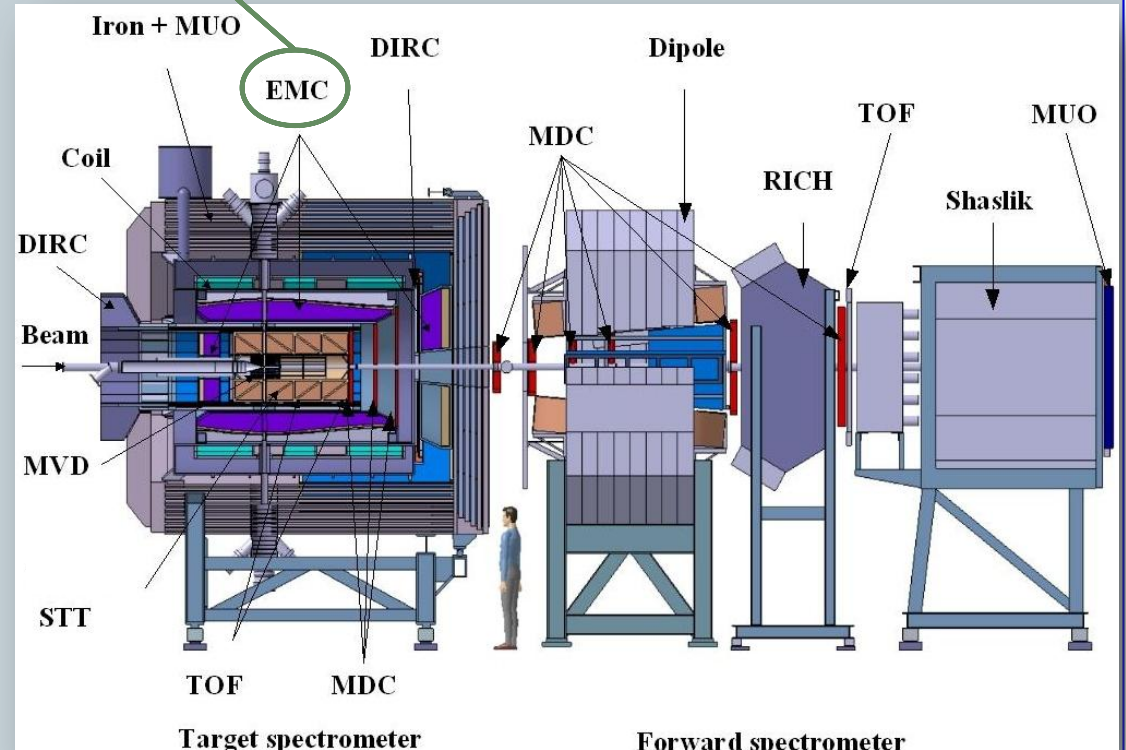

Detector requirements

- Nearly 4π solid angle
- High rate capability (2 10^7 interactions/s)
- Efficient event selection
- Momentum resolution (~2% at 1GeV)
- Good particle identification
- Vertex resolution below 100 μm

Electromagnetic calorimeter prototype

PWO EMC

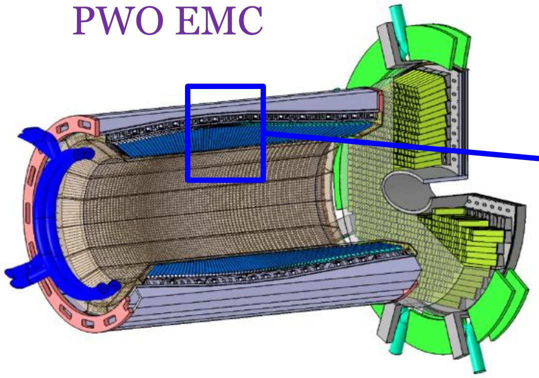

Lead tungstate (PWO) crystals
Cooled down to -25.0°C
Avalanche Photo Diodes for photon detection

Test of the 60 crystal prototype built at the IPN Orsay

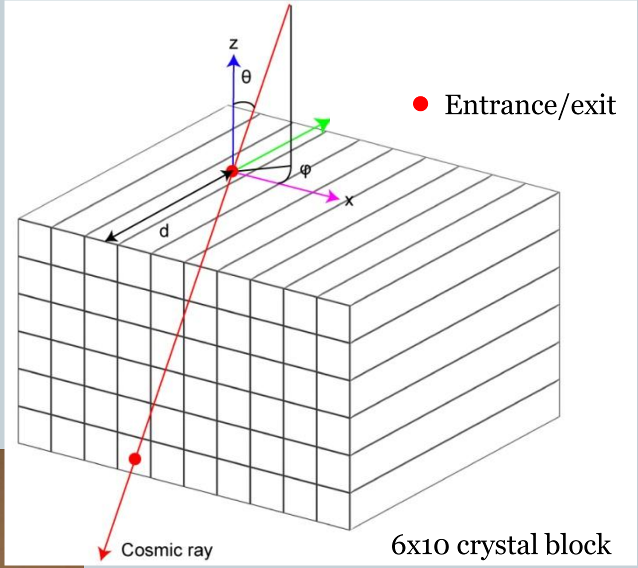

6x10 crystal block

Prototype crystals

Front face: 21.9x21.3 mm^2
Rear face: 27.5x27.3 mm^2
Length: 200 mm

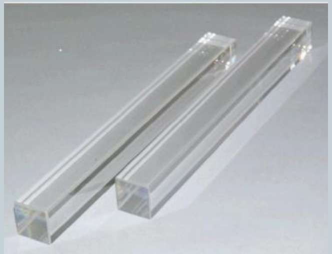

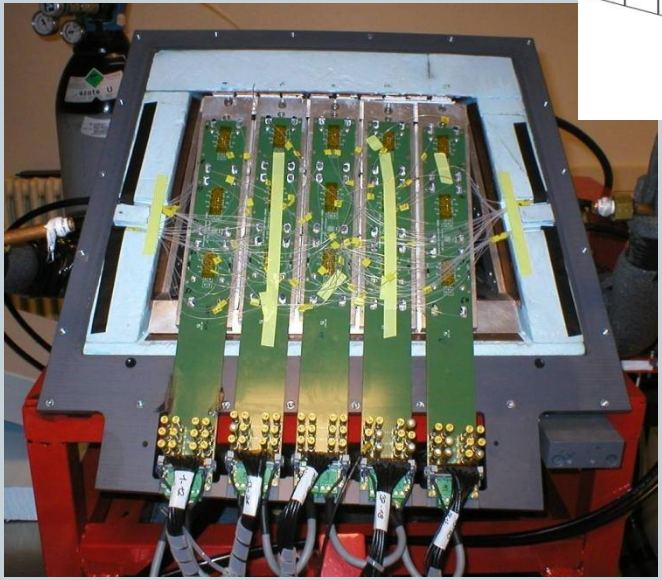

View of the prototype from the back

Electromagnetic calorimeter prototype

1. Calibration using cosmic rays

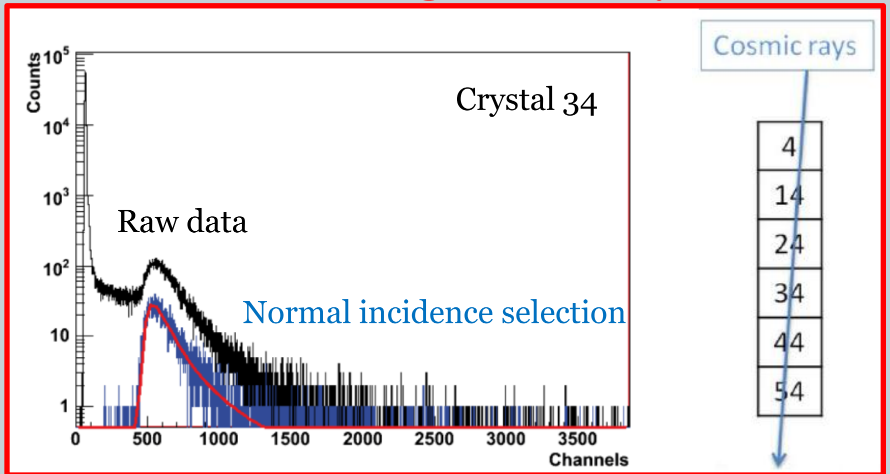

2. Linearity using MAMI C tagged photon beam

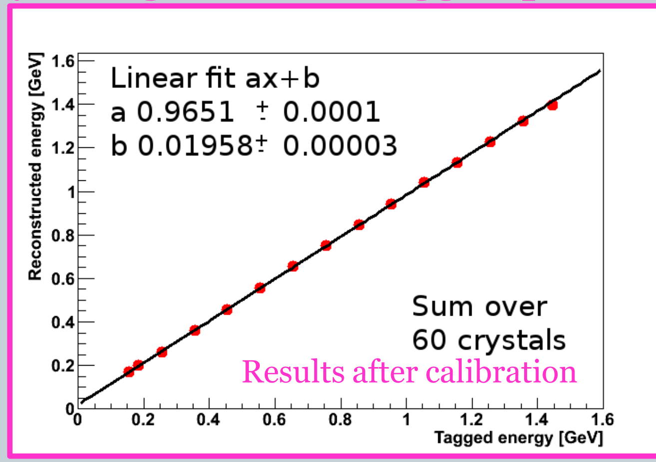

3. Resolution using tagged photon beam at MAMI C (Institut für Kernphysik, Mainz)

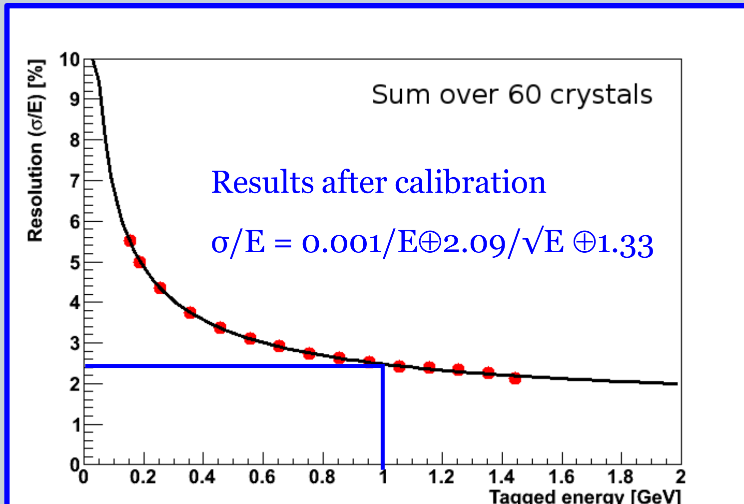

At E_γ=1GeV, σ/E=2.47%

General formalism for the e^+e^- production via one virtual photon exchange

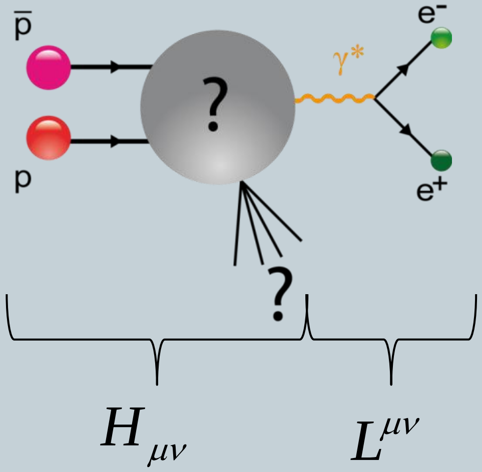

Differential cross section

$$d^{3n-4}\sigma \propto |M|^2 \propto \frac{1}{q^4} L^{\mu\nu} H_{\mu\nu}\left(s, q^2, \ldots\right)$$

Calculation by J. Van de Wiele

In the γ* rest frame (unpolarized experiment)

$$L^{\mu\nu} H_{\mu\nu} = 4e^2 \frac{q^2}{2}\left(H_{11} + H_{22} + H_{33}\right)$$

$$-8e^2 p_e^{*2}\left(H_{11} \sin^2\theta_e^* \cos^2\varphi_e^* + 2H_{12} \sin^2\theta_e^* \sin\varphi_e^* \cos\varphi_e^*\right.$$

$$+ 2H_{13} \sin\theta_e^* \cos\theta_e^* \cos\varphi_e^* + H_{22} \sin^2\theta_e^* \sin^2\varphi_e^*$$

$$\left. + 2H_{23} \sin\theta_e^* \cos\theta_e^* \sin\varphi_e^* + H_{33} \cos^2\theta_e^*\right)$$

The angular distribution in θ_e^* and φ_e^* gives access to 6 $H_{\mu\nu}$